THE JOURNAL OF COMPARATIVE NEUROLOGY 376:112–127 (1996)

Neurofilament Protein Is Differentially Distributed in Subpopulations of Corticocortical Projection Neurons in the Macaque Monkey Visual Pathways

PATRICK R. HOF, LESLIE G. UNGERLEIDER, MAREE J. WEBSTER, RICARDO GATTASS, MICHELLE M. ADAMS, CYNTHIA A. SAILSTAD, AND JOHN H. MORRISON

Fishberg Research Center for Neurobiology and Laboratories for Neurobiology of Aging (P.R.H., M.M.A., C.A.S., J.H.M.), and Departments of Geriatrics and Adult Development (P.R.H., J.H.M.), and Ophthalmology (P.R.H.), Mount Sinai School of Medicine, New York, New York 10029; Laboratory of Neuropsychology, National Institute of Mental Health (L.G.U., M.J.W., M.M.A.), Bethesda, Maryland 20892; Stanley Foundation Research Program, National Institute of Mental Health Neuroscience Center at St. Elizabeth's (M.J.W.), Washington, DC 20032; and Departamento de Neurobiologia, Instituto de Biofísica Carlos Chagas Filho, Universidade Federal do Rio de Janeiro (R.G.), Rio de Janeiro 21941-900, Brazil

ABSTRACT

Previous studies of the primate cerebral cortex have shown that neurofilament protein is present in pyramidal neuron subpopulations displaying specific regional and laminar distribution patterns. In order to characterize further the neurochemical phenotype of the neurons furnishing feedforward and feedback pathways in the visual cortex of the macaque monkey, we performed an analysis of the distribution of neurofilament protein in corticocortical projection neurons in areas V1, V2, V3, V3A, V4, and MT. Injections of the retrogradely transported dyes Fast Blue and Diamidino Yellow were placed within areas V4 and MT, or in areas V1 and V2, in 14 adult rhesus monkeys, and the brains of these animals were processed for immunohistochemistry with an antibody to nonphosphorylated epitopes of the medium and heavy molecular weight subunits of the neurofilament protein. Overall, there was a higher proportion of neurons projecting from areas V1, V2, V3, and V3A to area MT that were neurofilament protein-immunoreactive (57–100%), than to area V4 (25–36%). In contrast, feedback projections from areas MT, V4, and V3 exhibited a more consistent proportion of neurofilament protein-containing neurons (70–80%), regardless of their target areas (V1 or V2). In addition, the vast majority of feedback neurons projecting to areas V1 and V2 were located in layers V and VI in areas V4 and MT, while they were observed in both supragranular and infragranular layers in area V3. The laminar distribution of feedforward projecting neurons was heterogeneous. In area V1, Meynert and layer IVB cells were found to project to area MT, while neurons projecting to area V4 were particularly dense in layer III within the foveal representation. In area V2, almost all neurons projecting to areas MT or V4 were located in layer III, whereas they were found in both layers II–III and V–VI in areas V3 and V3A. These results suggest that neurofilament protein identifies particular subpopulations of corticocortically projecting neurons with distinct regional and laminar distribution in the monkey visual system. It is possible that the preferential distribution of neurofilament protein within feedforward connections to area MT and all feedback projections is related to other distinctive properties of these corticocortical projection neurons.

Indexing terms: corticocortical projections, cytoskeleton, feedforward and feedback projections, occipitoparietal and occipitotemporal pathways, primate visual system

The primate visual system contains over 25 cortical regions that can be identified by anatomical and physiological criteria. These restricted cortical domains contain independent representations of the visual field and are involved in the segregation and analysis of submodalities of the visual images. Sensory cues (e.g., form, color, and motion)

Accepted July 9, 1996.

Dr. Ungerleider's present affiliation is Laboratory of Brain and Cognition, National Institute of Mental Health, Bethesda, MD 20892.

Address reprint requests to Dr. Patrick R. Hof, Fishberg Research Center for Neurobiology, Box 1065, Mount Sinai School of Medicine, One Gustave L. Levy Place, New York, NY 10029-6574. E-mail: hof@cortex.neuro.mssm.edu

are processed by two divergent yet interactive sytems, the so-called magnocellular (motion) and parvicellular (form, color) pathways. Both pathways originate from discrete populations of retinal ganglion cells and remain partially segregated through a variety of association regions in the parietal and temporal cortex (Rockland and Pandya, 1979; Mishkin et al., 1983; Maunsell and Newsome, 1987; Gattass et al., 1986; Livingstone and Hubel, 1988; Zeki and Shipp, 1988; Morel and Bullier, 1990; Baizer et al., 1991; Felleman and Van Essen, 1991; DeYoe et al., 1994; Van Essen and Gallant, 1994). The fact that functional segregation occurs along these visual pathways may be reflected in a certain degree of morphological and biochemical specialization of the neurons of the projections from the occipital cortex to cortical areas that occupy a higher level in the hierarchical organization of visual processing, such as areas MT and V4. In this context, the combination of tract-tracing with immunohistochemistry allows for the identification of reliable neurochemical, connectional, and morphological criteria that can be used to define the particular phenotype of different subsets of corticocortically projecting neurons (Campbell et al., 1991; Hof et al., 1994, 1995a,b; Nimchinsky et al, 1996).

Previous analyses have demonstrated that pyramidal neurons containing high somatodendritic levels of neurofilament protein exhibit striking region-specific distribution patterns in the monkey visual cortex, permitting the definition of as many as 28 visual areas based on anatomical quantitative indices (Hof and Morrison, 1995). In addition, tract-tracing analyses have shown that the proportion of neurofilament protein-immunoreactive neurons among long association projections, as well as in visual pathways, is highly heterogeneous (Campbell et al., 1991; Hof et al., 1994, 1995b). Using the same antibody as in the present analysis, we have reported the distribution of neurofilament protein within subsets of corticocortically projecting neurons in long ipsilateral corticocortical pathways in comparison to short corticocortical, commissural, and limbic connections (Hof et al., 1995a). Long association pathways interconnecting the frontal, parietal, and temporal neocortex have a high representation of neurofilament protein-immunoreactive pyramidal neurons (45–90%), whereas short corticocortical, callosal, and limbic pathways are characterized by consistently fewer such neurons (4–35%). These differences in neurochemical phenotype of neurons furnishing corticocortical connections may have a considerable impact on cortical processing, and may be directly related to the type of integrative function subserved by each cortical pathway (Hof et al., 1995a). In this context, it is also interesting that neurofilament protein-immunoreactive neurons are dramatically affected in the course of Alzheimer's disease (Hof et al., 1990b; Hof and Morrison, 1990), suggesting that neurofilament protein may be crucially linked to the development of selective neuronal vulnerability and subsequent disruption of certain corticocortical pathways, which may be directly linked to the severe impairment of cognitive function commonly observed in age-related dementing disorders. It should also be kept in mind that neurofilament protein represents only one neurochemical marker used here to characterize pyramidal neuron subsets. For instance, immunohistochemical studies using an antibody to a chondroitin sulfate proteoglycan demonstrated that specific functional compartments and some of the visual areas in the magnocellular pathway can be identified by their high immunoreactivity to this component of the neuronal surface and extracellular matrix (DeYoe et al., 1990; Hockfield et al., 1990). However, these results are challenged by earlier reports (Hendry et al., 1984, 1988), demonstrating that this particular antigen may not be restricted to broad band neurons in the lateral geniculate nucleus and visual cortex in macaque monkeys as well as other species.

TABLE 1. Summary of Injection Sites[1]

Injections in areas MT and V4			Injections in areas V1 and V2		
Monkey	No of sites	Tracer	Monkey	No of sites	Tracer
RH1	2	DY	RH3	3	DY
	6	FB		6	FB
RH2	2	DY	RH5	11	DY
	6	FB		13	FB
RH4	10	FB	RH6	9	FB
	11	DY		9	DY
RH7	14	DY	RH9	13	DY
	12	FB		16	FB
RH8	15	FB	RH10	16	DY
	10	DY		11	FB
RH11	22	FB	RH13	15	FB
	13	DY		13	DY
RH12	15	DY	RH14	19	FB
	9	FB		15	DY

[1]Each cortical injection consisted of several sites that each received 200 nl to 1 μl of Fast Blue (FB) or Diamidino Yellow (DY). The injection sites were physiologically mapped in animals RH1, RH2, and RH3 and these data were subsequently used to guide the placement of injections. For both sets of injections, the first line represents the number of injection sites and tracer injected in areas MT or V1, and the second line represents areas V4 or V2, respectively. See Materials and Methods and Fig. 1 for details.

In the present study, we analyzed the distribution neurofilament protein-immunoreactive neurons in several feedforward and feedback visual projections following injections of retrograde tracers in areas V1, V2, V4, and MT in macaque monkeys, in order to define further the neurochemical features of neurons participating in corticocortical pathways subserving well defined visual functions, and to assess the degree to which this cellular neurochemical feature may be related to certain physiologic aspects of sensory processing in these identified sets of projections. Preliminary data from this study have been reported in abstract form (Kupferschmid et al., 1991, 1992; Hof et al., 1994, 1995b).

MATERIALS AND METHODS

Surgical procedures

Fourteen adult Rhesus monkeys (*Macaca mulatta*) were used in the present study (Table 1). Materials from these animals were used in previous studies of the macaque visual system as well (Hof et al., 1994, 1995a,b; Hof and Morrison, 1995), and all experimental protocols were conducted within NIH guidelines for animal research and were approved by the Institutional Animal Care and Use Committee (IACUC) at both Mount Sinai School of Medicine and NIH. Eleven out of 14 animals received relatively large injections of the retrograde tracers Fast Blue (FB) and Diamidino Yellow (DY) in either the mediotemporal area MT and area V4, or in areas V1 and V2, whereas three animals, in which the visuotopic loci of the injection sites were mapped physiologically, received smaller injections (Table 1; Fig. 1). The retrograde tracers were injected in order to include extensive portions of the areas of interest in each animal (Fig. 1). Also, depending on the animal, FB and DY were used alternatively in areas MT and V4 (or V1 and V2), so that the same tracer was not used consistently at the same injection site (Table 1). The areas chosen for injections have been extensively characterized physiologically, their location can be easily identified using sulcal and

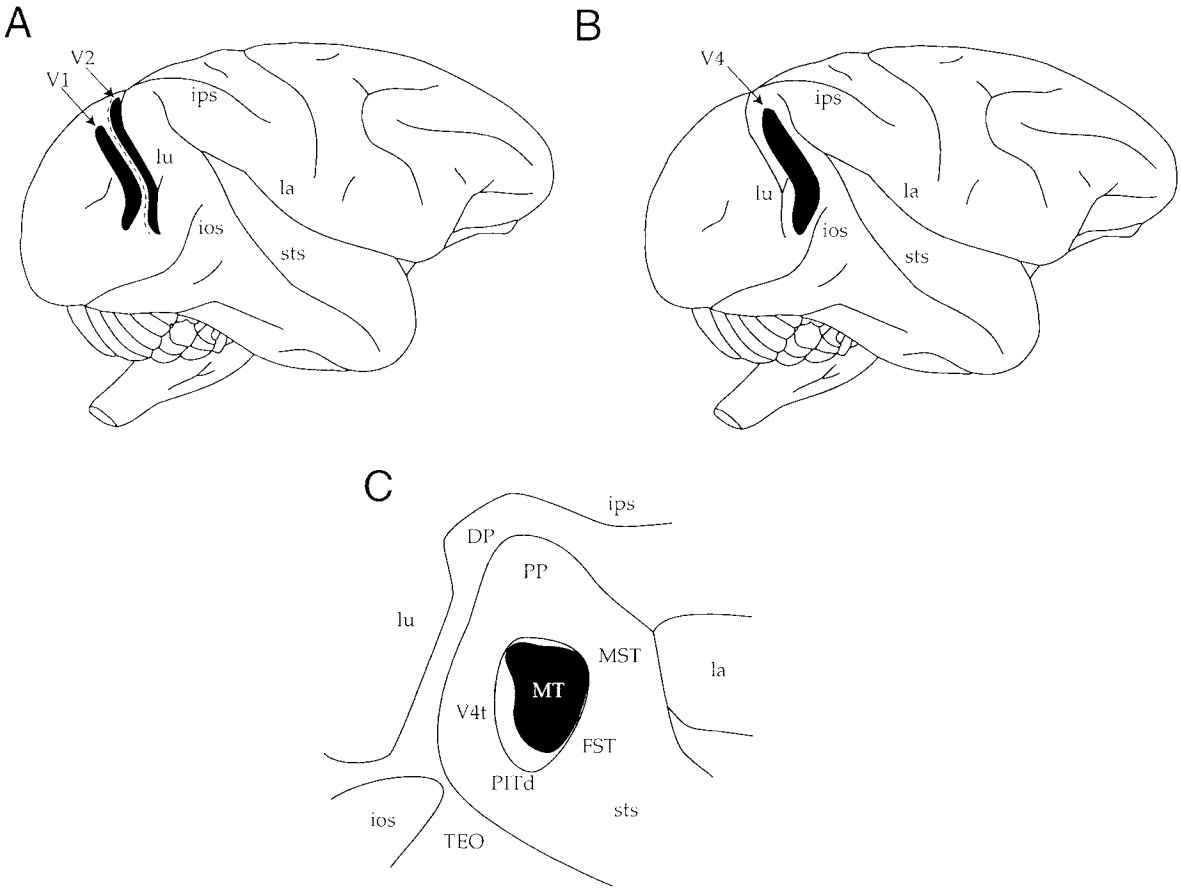

Fig. 1. Schematic representation of the localization and size of injections in areas V1 and V2 (**A**), V4 (**B**), and MT (**C**). The black areas indicate the maximal spread of the tracers and represent the total area injected in all of the monkeys combined. In each animal, the injections were restricted to the cortical areas of interest. In C, the lateral (la), lunate (lu), intraparietal (ips), superior temporal (sts), and inferior occipital (ios) sulci have been artificially opened to demonstrate the approximate location of the middle temporal (MT) and adjacent areas (indicated by upper case lettering). In animals with injections in areas V1 and V2, tracers were placed in regions corresponding to the central visual field representation (A). In all animals, tracer injections covered large portions of areas V4 and MT (B, C). DP, dorsal prelunate area; FST, fundal superior temporal area; MST, medial surperior temporal area; PITd, posterior inferior temporal cortex, dorsal part; PP, posterior parietal area; TEO, temporo-occipital cortex; V4t, transition region between areas V4 and MT.

gyral landmarks, and are easily exposed surgically (Zeki, 1974; Ungerleider and Mishkin, 1979; Gattass and Gross, 1981; Van Essen et al., 1981; Ungerleider and Desimone, 1986; Felleman and Van Essen, 1987; Gattass et al., 1988).

Animals were tranquilized with ketamine hydrochloride (25 mg/kg i.m.), intubated, and maintained under halothane general anesthesia (0.5–1.5% as necessary in air), and strict sterile surgical conditions. They were placed for surgery in a custom designed large animal head holder. After deinsertion and reflection of the temporal muscle, a craniotomy was performed over the cortical site, and the dura mater was incised and reflected. Up to 22 injections (200 nl each) of 4% aqueous solutions of either FB or DY were placed within the cerebral cortex by using a 1 μl Hamilton microsyringe with a 24 gauge needle (Table 1; Fig. 1). In the case of area V4, injections were placed along a descending line starting approximately 2–3 mm below the junction of the superior temporal and intraparietal sulci to avoid the dorsal prelunate area DP, and extended about 1 mm along the posterior border of the inferior occipital sulcus ventrally to end above the anterior extension of areas V2 and VP. To inject area MT, the cortex of the dorsal bank of the posterior portion of the superior temporal sulcus was surgically aspirated, and tracer injections were then placed in the floor of the sulcus. Injections in area V2 were placed along the posterior margin of the lunate sulcus, with special care to avoid spreading of the dye in the subcortical white matter. The location of the boundary between areas V2 and V1 was easily recognized from the surface, and the proper placement of the injections within the cortex was further ascertained on cross-sections. Injections in area V1 were placed in a vertical strip of opercular cortex along the V1/V2 border, which comprised the V1's foveal representation as well as parafoveal portions of the inferior visual hemifield. All of the injections were verified anatomically. In three animals (RH1, RH2, and RH3), injections sites were located by electrophysiological mapping techniques, and these data were used as guides in the subsequent experiments. For these animals, after a desired injection site was identified, a guide tube was advanced through the dura and placed about 300 μm above the intended site. A microelectrode was then advanced through the guide tube and the visuotopic location of the injection site was confirmed. The electrode was then withdrawn from

the guide tube and replaced by 1 μl Hamilton syringe. Using 0.02 μl steps we injected 1 μl of DY in area MT and 0.3 μl of FB in area V4 for each injection site in animals RH1 and RH2. Similarly, monkey RH3 received 1 μl of FB in area V2 and 0.3 μl of DY in area V1 for each injection site (Table 1). To minimize leakage of the tracer into the electrode track, the syringe was left in place for 20 minutes following injections.

Tissue preparation and staining procedure

Following surgery, a survival time of 21 days was set to allow for reliable retrograde transport of FB and DY as described in our previous studies (Kuypers and Huysmans, 1984; Campbell et al., 1991; Hof et al., 1995a). Then, the animals were perfused as previously described (Hof and Nimchinsky, 1992; Hof et al., 1995a; Hof and Morrison, 1995). Briefly, the animals were deeply anesthetized with ketamine hydrochloride (25 mg/kg i.m.) and sodium pentobarbital (20–35 mg/kg i.v., as necessary), intubated and mechanically ventilated. The chest was then opened, the heart exposed, and 1.5 ml of 0.1% sodium nitrite was injected into the left ventricle. The descending aorta was clamped and the monkeys were perfused transcardially with cold 1% paraformaldehyde in phosphate buffer for 1 minute followed by cold 4% paraformaldehyde for 10 to 12 minutes. The brains were then removed from the skull, cut into 4–10 mm-thick coronal blocks, postfixed for 6 to 7 hours in 4% paraformaldehyde at 4°C, and cryoprotected in a series of graded sucrose solutions (12, 16, 18, and 30%) in phosphate-buffered saline (PBS). For histological and immunohistochemical purposes, the blocks were frozen on dry ice following postfixation and cryoprotection, and adjacent 40 μm-thick sections were cut from the coronal blocks on a sliding microtome or on a cryostat. In all of the animals, the sections from each block were kept in anatomical series and every tenth section was processed for immunohistochemistry. The remaining sections were cryoprotected and stored in serial order at -20°C.

Monoclonal antibody SMI-32 (Sternberger Monoclonals, Baltimore, MD), that recognizes nonphosphorylated epitopes on the medium (168 kDa) and heavy (200 kDa) molecular weight subunits of the neurofilament protein (Sternberger and Sternberger, 1983; Lee et al., 1988) was used in the present analysis. For immunohistochemistry, 40-μm-thick free-floating sections were incubated for 48 hours at 4°C with the monoclonal antibody SMI-32 at a dilution of 1:5,000 in PBS containing 0.3% Triton X-100 and 0.5 mg/ml bovine serum albumin. The sections were then processed using a biotinylated secondary antibody and fluorescein-conjugated avidin D, mounted onto glass slides, and coverslipped with Permafluor. This method was found to yield an optimal immunofluorescence signal. A parallel series of sections was stained for brightfield microscopy and processed with the avidin-biotin method using a Vectastain ABC kit (Vector Laboratories, Burlingame, CA) and 3,3'-diaminobenzidine as a chromogen. In this case SMI-32 immunoreactivity was subsequently intensified in 0.005% osmium tetroxide (Fig. 2). In all of the animals, additional series of sections were stained with cresyl violet in order to clarify the cytoarchitecture and reconstruct the injection sites.

Regional and laminar analyses

Analyses of the distribution of retrogradely and double labeled neurons were performed using a computer-assisted image analysis system consisting of a Zeiss Axiophot photomicroscope equipped with a Zeiss MSP65 computer-controlled motorized stage (Zeiss, Oberkochen, Germany), high sensitivity SIT666 TV scanner (DAGE MTI, Michigan City, IN) or Zeiss ZVS-47E (Zeiss, Thornwood, NY) video camera system, a Macintosh 840AV workstation, and NeuroZoom morphometry software developed in collaboration with the Scripps Research Institute (La Jolla, CA; Young et al., 1995; Bloom et al., 1996; Nimchinsky et al., 1996). Materials were analyzed by using fluorescence lighting conditions with a Zeiss Plan Neofluar 20X and 40X objectives, a Zeiss UV filter to detect FB, and DY-containing retrogradely labeled neurons or narrow bandpass fluorescein filter sets to visualize neurofilament protein immunoreactivity.

In each animal, every other section from the original series stained with antibody SMI-32 (i.e., a 1 in 20 series), was systematically counted. The regional and laminar numbers of retrogradely and double labeled neurons projecting to areas V4 and MT were recorded in layers II–III and V–VI separately, in areas V2, V3, and V3A. In area V1, retrogradely labeled layers III and IVB neurons, as well as Meynert cells were counted as separate neuronal populations. Similarly, after tracer injection in areas V1 and V2, retrogradely labeled cells were counted in layers II–III and V–VI of areas V3, V4, and MT. The analyses were performed on a digitized image for each field of interest. In each animal, neurons that were single labeled (i.e., containing FB or DY only) and double labeled (i.e., containing one of the retrograde tracers and immunolabeled by antibody SMI-32) were counted simultaneously by switching the filter combinations in 10 to 15 sections depending on the animal, in layers II–III and V–VI, separately. The computer graphics were then superimposed on the digitized image. The position of each neuronal profile of interest was registered and labeled differently on the computer maps, so that the numbers of retrogradely labeled neurons and the proportion of double labeled neurons within a given projection (i.e., the percentage of double labeled neurons calculated from total retrogradely labeled neuron counts) to areas MT and V4, or V1 and V2, could be estimated with a laminar level of resolution. With respect to the quantification of the numbers of retrogradely and double labeled neurons, it should be noted that we did not use a stereologic approach. Although it is true that systematic random sampling would yield robust estimates of neuron numbers (Sterio, 1984; Gundersen and Jensen, 1987; West et al., 1991), the biological and experimental variability in tract-tracing experiments is such that it would make the stereologic analysis of a given projection (using, for example, an optical fractionator) extremely cumbersome, and potentially not totally meaningful (for example, in the present study the injections in areas MT and V4 yielded consistently lower numbers of retrogradely labeled neurons compared to the injections area V1 and V2; such factors cannot be controlled for and may lead to misinterpretation of stereologic data). The present analysis did show, however, consistency in the data in that percentages of double labeled neurons were comparable among animals, even though the raw counts of retrogradely (and double) labeled neurons varied greatly. The point of the present analysis being the expression of the percentage of neurons containing neurofilament protein in several corticocortical pathways, we did not feel it necessary to undertake a formal stereologic assessment of the total number of neurons participating in

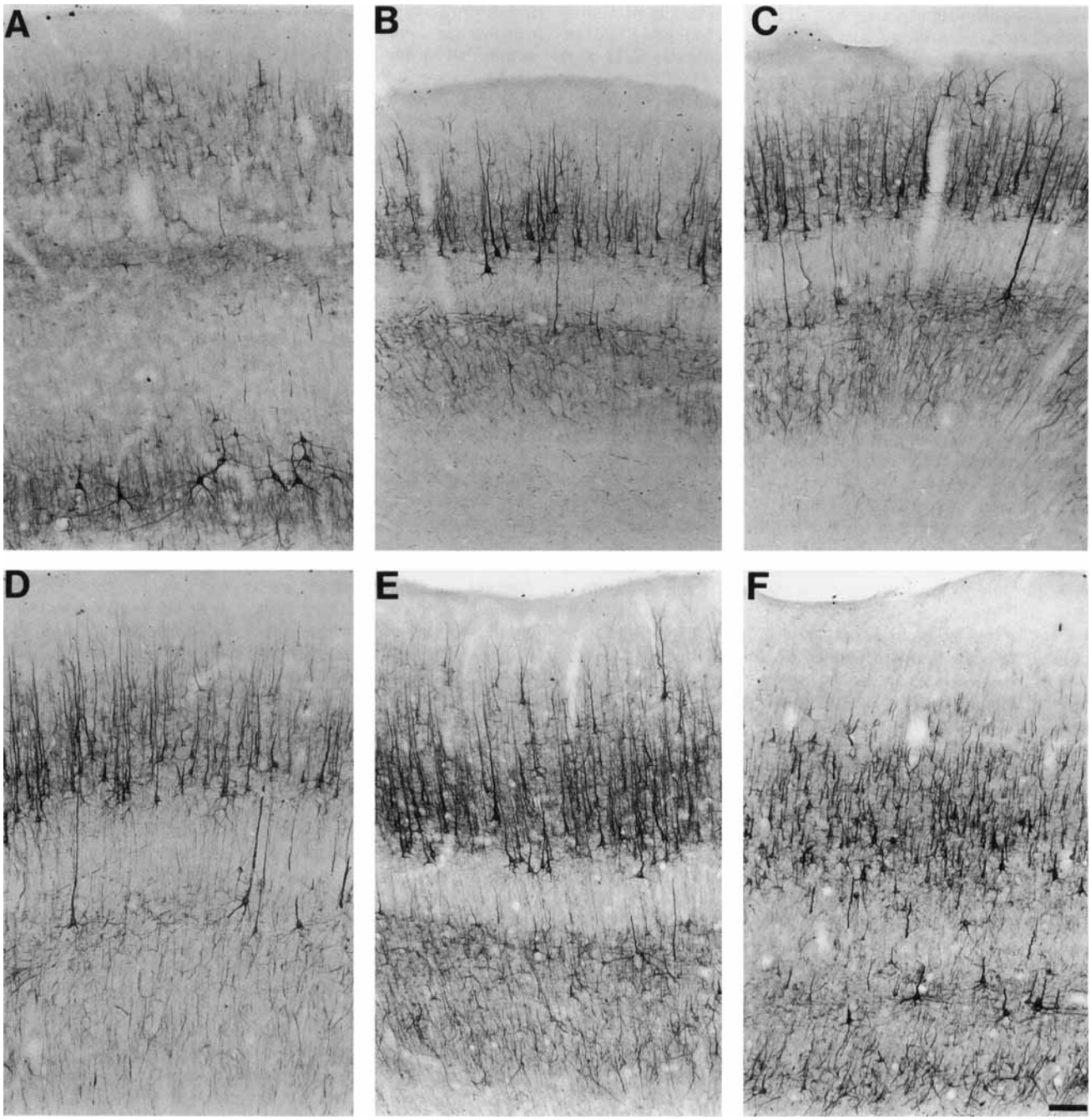

Fig. 2. Distribution of neurofilament protein in areas V1 (**A**), V2 (**B**), V3 (**C**), V3A (**D**), V4 (**E**), and MT (**F**). There are clear laminar patterns of labeled neuron distribution among these areas. Note the prominent staining of large pyramidal neurons, including Meynert cells and layer IVB in area V1 (A), layer III and V neurons in areas V2, V3, and V3A (B–D), the denser and generally lighter pattern as well as layers II-superficial III neurons observed in area V4 (E). Some conspicuous layer II neurons are labeled in area V3 (C). Area MT contains large layer III and V cells and a distinct band of immunoreactive neurons in layer VI (F). Scale bar = 100 μm.

these projections, at the laminar level. In all cases, it should be noted that we made sure to survey and quantify adequately the retrogradely labeled neurons, in comparable series of immunoreacted sections that encompassed the entire extent of the cortical region investigated. This avoided a certain degree of bias due to clustering of data collection to only parts of a given cortical area.

In addition, accurate maps were electronically constructed by assembling a series of counting frames to show the distribution of labeled profiles in large areas consisting of several adjacent microscopic fields (Hof et al., 1995a; Young et al., 1995; Nimchinsky et al., 1996). The coordinates of each labeled element were recorded in each microscopic field, typically a fraction of a cortical layer, relative to

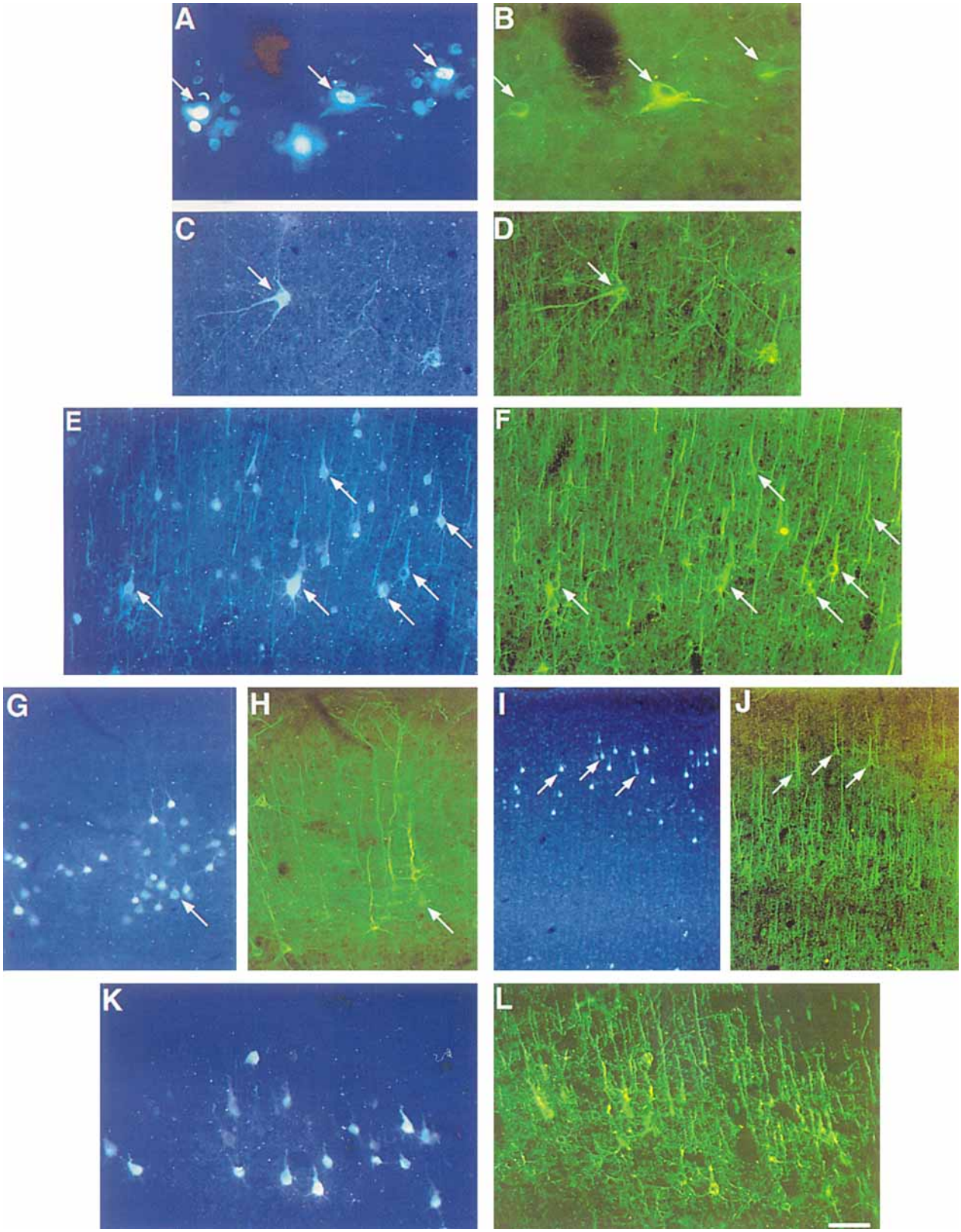

Fig. 3. Examples of retrogradely labeled and neurofilament protein-immunoreactive double labeled neurons in feedforward and feedback visual projections. Each pair of photomicrographs represents the same field. Layer IVB neurons (**A, B**) and Meynert cells (**C, D**) in area V1 following DY (A, B) or FB (C, D) injections in area MT. All retrogradely labeled neurons are enriched in neurofilament protein (arrows). Panels **E–H** show layers II-III of area V2 following FB injections in areas MT (**E, F**) or V4 (**G, H**). Note the lower density of double labeled neurons in the case of the injection in area V4 (arrows, E–H). Panels **I** and **J** show retrograde labeling of layers II and IIIA neurofilament protein-containing neurons in area V3 after injection of FB in area V4. There are several double labeled neurons in layers II and IIIA (arrows, I–J). Panels **K** and **L** show examples of retrogradely labeled neurons in area MT after injection of area V1. There is a large number of double labeled neurons in layers V and VI. These computer generated photomicrographs were obtained by scanning the original photographic slides on a Agfa Arcus II high resolution scanner. The plate was subsequently prepared with Adobe Photoshop software and printed on a color laser printer. No alterations were made to the original materials except that some of the original color intensity was lost during printing. Scale bar = 100 μm in L (and applies to C–H, K), 75 μm (for A, B), 200 μm (for I, J).

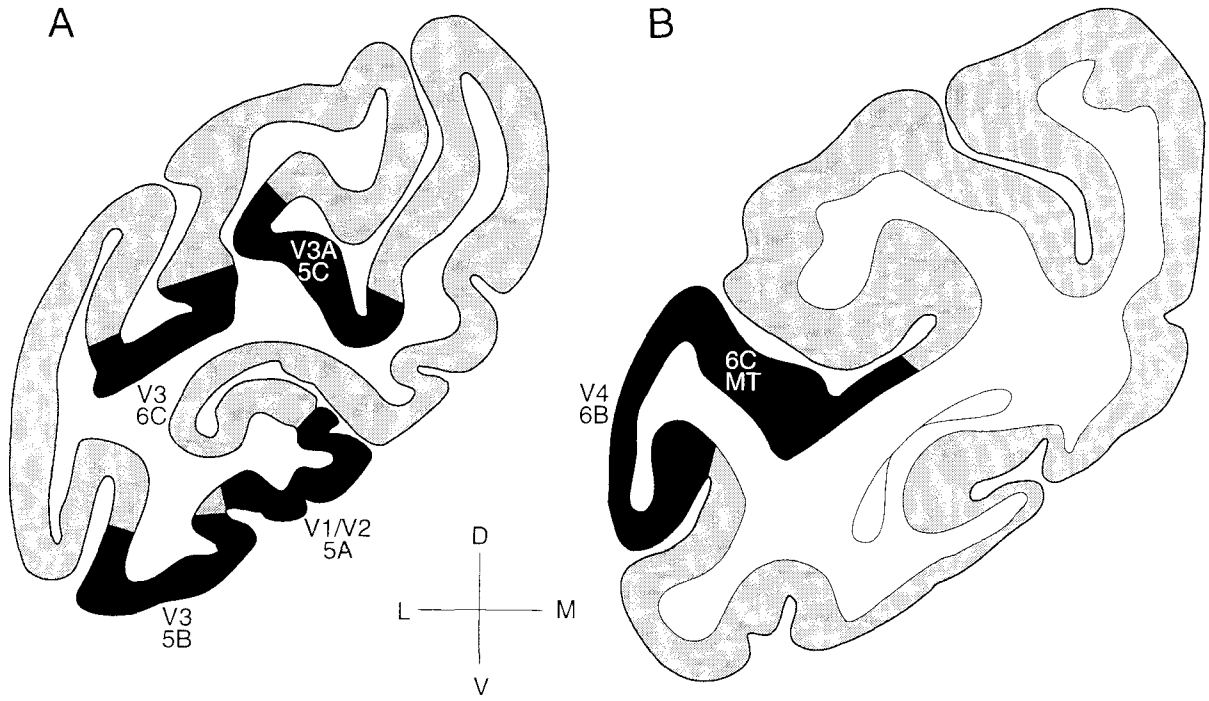

Fig. 4. Schematic representations of the areas mapped in Figures 5 and 6. The relevant sections were traced by using a computer-assisted morphometry system (NeuroZoom, Young et al., 1995), and the location of the cortical maps enlarged in the following figures highlighted (black zones). Each location is designated by its corresponding number on Figures 5 and 6.

an origin, and the map was automatically assembled. Laminar boundaries were created by editing the map at the same time data were collected. The accuracy of laminar boundaries was further ascertained on adjacent non-fluorescence sections stained with the antibody SMI-32 and on Nissl preparations (Fig. 2). Overall, the topographic localization of 23,145 retrogradely labeled and 14,561 double labeled neurons was recorded in the present analysis. The data were calculated in each animal separately, in view of substantial discrepancy in the numbers of retrogradely and double labeled neurons across animals resulting from differences in the amount of tracers injected in the areas of interest. In spite of interindividual variability, the percentages of double labeled neurons relative to the number of retrogradely labeled neurons in each injection paradigm was generally consistent for each marker analyzed. Therefore, percentages of double labeled neurons calculated from laminar data were pooled across all of the animals for each of areas MT and V4 injections, or areas V1 and V2 injections. Due to the differences in injections in areas MT and V4, analyses concentrated in most cases to regions of topographic overlap. Also, since the distribution patterns of retrogradely labeled neurons in the dorsal and ventral parts of area V3 and in area V3A were qualitatively comparable, results from these regions were pooled in the quantitative analysis and referred to as V3. Data from the different projections are shown graphically on Figures 5 and 6, and the schematic drawings on Figure 4 indicate the location of each computer-generated map. The statistical analysis was performed using a one-way analysis of variance to assess possible differences in the proportions of double labeled neurons among the cases. Similarly, an analysis of variance was used to demonstrate differences in the proportions of double labeled neurons among the cortical regions of origin of the projections considered. Subsequently, differences among specific layers and cortical regions were assessed using multiple comparisons of the means according to the Student-Newman-Keuls method (Sachs, 1984).

RESULTS

Regional patterns of neurofilament protein distribution

Neurofilament protein-immunoreactive neurons exhibited a very high degree of regional heterogeneity across cortical areas. The distribution of neurofilament protein in the monkey visual system corresponded to that reported in a previous analysis (Hof and Morrison, 1995). In summary, the majority of neurofilament protein-enriched neurons are medium to large size pyramidal neurons with extensive

Fig. 5. Representative computer-generated maps of the distribution of retrogradely labeled (blue open circles) and double labeled (red stars) neurofilament protein-immunoreactive neurons in areas V1, ventral V2 (**A**), ventral V3 (**B**), that project to area MT, and from area V3A to areas V4 and MT (**C**). On panel C, the neurons projecting to area V4 are coded as in panels A and B, whereas retrogradely labeled cells projecting to area MT area shown by yellow squares and double labeled cells projecting to area MT by green circles. All of the retrogradely labeled neurons in the projection from area V1 to MT display neurofilament protein immunoreactivity, whereas the projections from areas V2 and V3 have slightly lower densities of double labeled neurons (A, B). Note that the projection from areas V3A to V4 displays fewer double labeled neurons than that to MT (C). In panel C, note the intervening patterns of projection neurons to areas V4 and MT. Maps A and B are from animal RH12, C is from animal RH8. Scale bars = 1 mm.

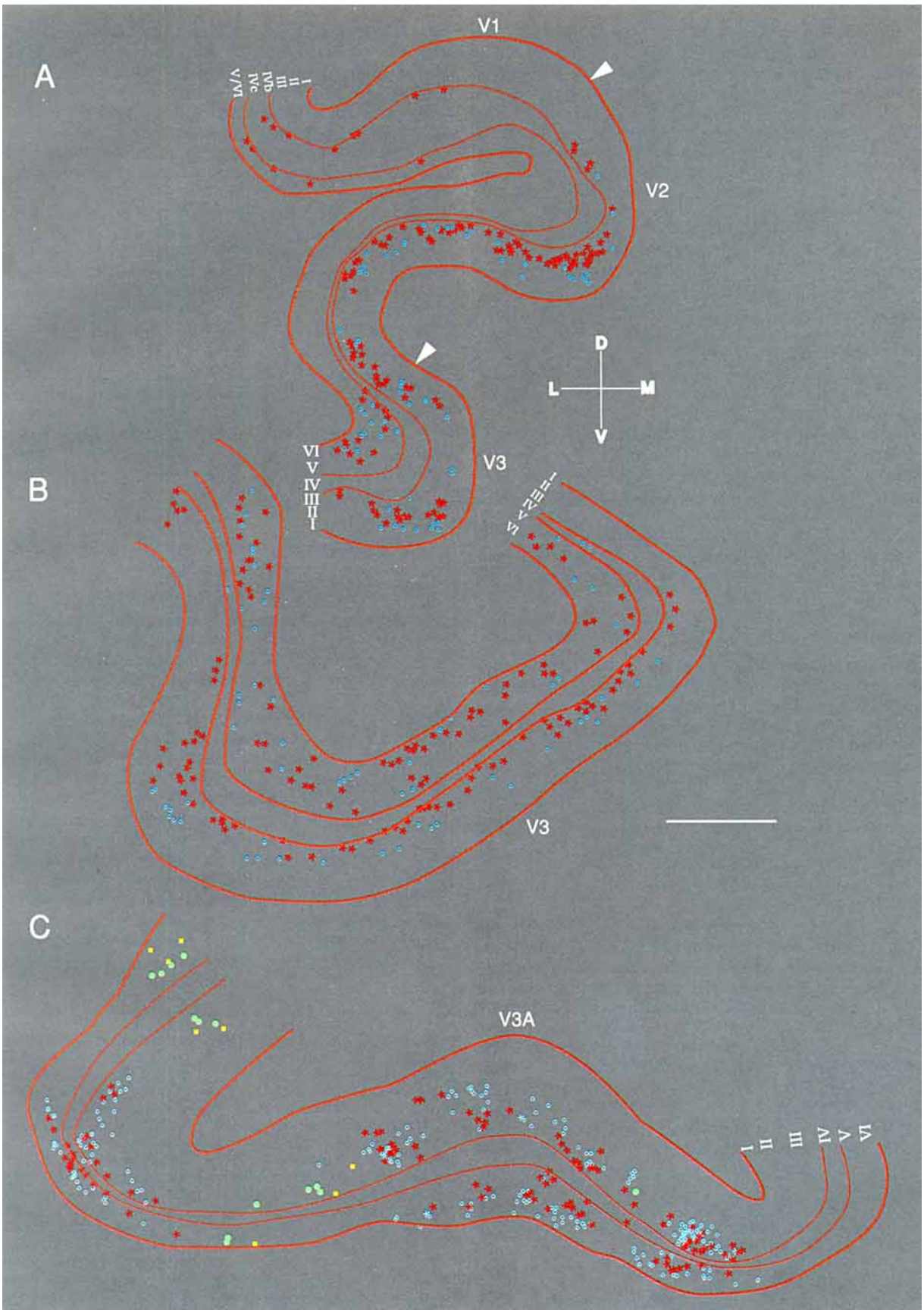

Figure 5

basal and apical dendritic arborizations (Campbell and Morrison, 1989; Hof and Morrison, 1995). In area V1, they were present in moderate densities in layers II, III, and V, almost absent in layer IVC, while layer VI contained a consistent population of relatively small, lightly stained pyramidal and fusiform neurons. The large layer IVB neurons and the Meynert cells at the border between layers V and VI were intensely labeled (Fig. 2A). Area V2 was characterized by a dense band of large, darkly labeled pyramidal neurons located in the lower two thirds of layer III and a much sparser population of large neurofilament protein-immunoreactive neurons in layer V and smaller, lightly labeled neurons in layer VI (Fig. 2B). Area V3 was characterized by the presence of small neurofilament protein-immunoreactive neurons in layers II and IIIA, and in the superficial portion of layer III (Fig. 2C). This pattern was not observed in areas V1 and V2. Layer III of area V3 contained slightly lower densities of labeled pyramidal neurons than area V2, whereas the number of smaller lightly stained neurons in layers V-VI was higher in areas V3 and V3A. The large layer V pyramidal neurons were very conspicuous in areas V3 and V3A (Fig. 2C, D). Area V4 had considerably higher numbers of neurofilament protein-positive neurons in layers V and VI than did area V3 (Fig. 2E), and area MT was characterized by the presence of very large, regularly spaced immunoreactive neurons in layer V and a distinct band of intensely labeled, small neurons in layer VI that clearly demarcated this region from area V4 (Fig. 2F).

Distribution of retrogradely labeled neurons

Feedforward projections. Although variability in the amount of tracers injected in the areas in each experimental animal resulted in variability in the density of retrogradely labeled cells among the projections analyzed, all injections in areas V4 and MT yielded consistent qualitative patterns of retrograde labeling distribution in areas V1, V2, V3, and V3A. In area V1, injections in area V4 resulted in the labeling of a restricted, dense population of retrogradely labeled neurons in layers II and III of the opercular region corresponding to the V1's foveal representation (Daniel and Whitteridge, 1961; Zeki, 1978; Yukie and Iwai, 1985), as well as the labeling of layer III neurons scattered throughout the rest of the area. Injections in area MT resulted in retrograde labeling of generally restricted subsets of large layer IVB neurons and Meynert cells that were observed in higher numbers in the calcarine cortex than in the opercular cortex (Figs. 3A–D, 5A, B). Retrograde labeling occurred in both the dorsal and ventral portion of areas V2 and V3, as well as in area V3A. In area V2, retrograde labeling from both areas V4 and MT was almost entirely confined to large layer III pyramidal neurons (Figs. 3E–H, 5A, B). In both areas V3 and V3A, retrogradely labeled neurons were found in both layers II–III and V–VI, with comparable or slightly higher densities in the supragranular layers (Fig. 5B, C), and retrogradely labeled neurons were principally large layer III and medium size layer V pyramidal cells, although in several fields many labeled fusiform and small pyramidal neurons were seen in layer VI. Some small pyramidal neurons in layer II were also retrogradely labeled following injections in area V4 (Fig. 3I, J). Interestingly, retrogradely labeled neurons frequently presented as well defined non-overlapping patches of FB- and DY- containing cells in layers II–III of area V2, possibly conforming to functional cortical domains as described in the physiologic and anatomic study of Munk et al. (1995). More variable domains of mutually exclusive FB and DY retrograde transport were also found in layers III and V–VI of V3 and V3A.

Feedback projections. Qualitatively comparable patterns of retrogradely labeled neuron distribution in areas MT, V4, and V3 were observed across all experimental animals that received injections in areas V1 and V2. Injections in areas V1 and V2 resulted in labeling of a large population of feedback projection neurons predominantly located in layers V and VI in area MT and V4 (Figs. 3K, L, 6A, B). In these areas, layers II and III contained a relatively smaller number of retrogradely labeled neurons. In area V3, however, retrogradely labeled neurons were observed in comparable densities in both supragranular and infragranular layers (Fig. 6C). Retrogradely labeled neurons were mostly medium size pyramidal cells in layers III and V, while in layer VI many fusiform or horizontally oriented neurons, as well as smaller pyramidal cells were observed. In area V3, retrogradely labeled cells from areas V1 and V2 formed two large distinct patches on the anterior wall of the lunate sulcus, with the projection to area V1 situated dorsally to that to area V2 (Fig. 6C). In both areas V4 and MT, feedback projection neurons to areas V1 and V2 did not show segregation patterns in either layers II–III or V–VI (Fig. 6A, B).

Proportions of retrogradely and double labeled neurons

The regional and laminar distribution patterns of retrograde labeling in areas V1, V2, V3, and V3A indicated a substantial level of neurochemical specialization, among the neurons of origin of the projections to areas V4 and MT. In contrast, it appeared that feedback projections from areas V3, V4, and MT were far more homogeneous with respect to their content of neurofilament protein. In order to characterize more precisely these different neuronal subsets, the proportion of neurons containing neurofilament protein was quantitatively assessed for each projection. This analysis demonstrated that despite the variability in numbers of retrogradely labeled neurons, the proportions of double labeled neurons (i.e., retrogradely labeled and neurofilament protein-immunoreactive) were remarkably consistent among animals (Tables 2, 3). It should be noted that injections in areas MT and V4 yielded lower numbers of retrogradely labeled neurons than those placed in areas V1 and V2 (see Figs. 5, 6). This may be due to the fact that overall smaller amounts of the tracers were

Fig. 6. Representative computer-generated maps of the distribution of retrogradely labeled and double labeled neurofilament protein-immunoreactive neurons in areas MT (**A**), V4 (**B**), and V3 (**C**) that project to areas V1 and V2. In panels A and B, retrogradely labeled neurons projecting to area V1 are coded by blue dots and double labeled neurons projecting to area V1 by green dots. The projecting neurons to area V2 are similarly coded by salmon crosses and red stars, respectively. In panel C, the projection to area V2 appears as salmon and red dots, respectively. The pink dots or squares represents neurons projecting to both areas V1 and V2; all of these neurons also contained neurofilament protein. Note that the distribution of the labeled neurons is coextensive in areas MT and V4, whereas it is more segregated in V3. Most of the feedback projections in areas MT and V4 originate in layers V and VI, while they are equally distributed across supragranular and infragranular layers in area V3. There is a relatively homogeneous pattern of distribution of double labeled neurons among feedback projections in comparison to feedforward projections (Fig. 5). Maps A and B are from animal RH13, C is from animal RH14. Scale bars = 1 mm.

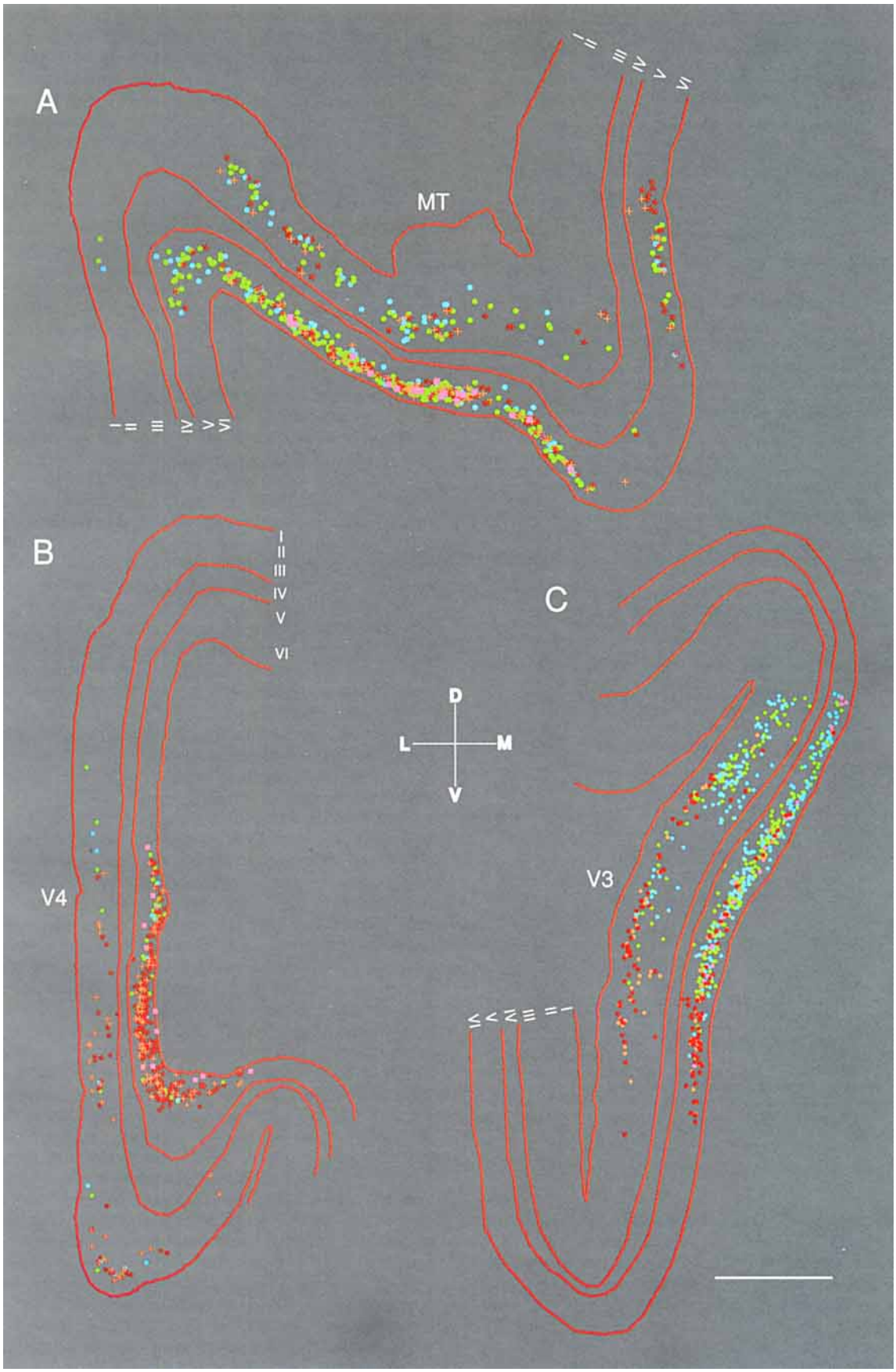

Figure 6

TABLE 2. Distribution of Neurofilament Protein-Immunoreactive Neurons in Corticocortical Projections to Areas MT and V4[1]

Source area	Monkeys							
	RH1	RH2	RH4	RH7	RH8	RH11	RH12	Mean
Projections to area MT								
Area V1								
Layer IVB	100	100	100	100	100	100	100	100
MC	100	100	100	100	100	100	100	100
Area V2								
Layers II–III	77.0	67.2	67.2	80.0	85.1	87.5	82.0	78.0 ± 2.8
Area V3								
Layers II–III	75.2	72.6	69.2	74.4	74.5	77.2	80.4	74.8 ± 1.2
V–VI	58.1	53.1	48.2	38.1	39.5	75.5	68.4	57.2 ± 3.8
Projections to area V4								
Area V1								
Layers II–III	20.0	35.0	24.1	20.0	30.0	25.0	21.4	25.1 ± 2.0
Area V2								
Layers II–III	47.5	42.1	26.6	21.2	21.2	39.3	27.7	32.2 ± 3.7
Area V3								
Layers II–III	45.8	49.2	27.9	27.5	26.8	40.8	33.0	35.9 ± 3.3
V–VI	31.4	44.8	24.4	16.3	13.2	35.7	33.3	28.4 ± 3.9

[1]Results represent the laminar percentages of double labeled neurons (i.e., retrogradely labeled and neurofilament protein-immunoreactive) in the projections from areas V1, V2, and V3 to the injections sites in areas V4 and MT. The mean ± S.E.M. percentages from all 7 animals is also indicated. No distinction was made between the ventral and dorsal portions of areas V2 and V3, and data from area V3A were included with those from area V3. Note that layer IVB and Meynert cells (MC) in area V1 that project to area MT were all double labeled. Also there is a much higher percentage of double labeled neurons in the occipitoparietal pathway (to area MT) than in the occipitotemporal pathway (to area V4). There was a very small number of neurons in layers V–VI of area V2 projecting to either areas V4 or MT, and among these neurons few were double labeled (10–20%). A few neurons projecting to both areas V4 and MT were observed exclusively in layers III and V of area V3A, and were consistently neurofilament protein-immunoreactive (97.1%). Animals are coded as in Table 1. See Results and Fig. 7 for details.

TABLE 3. Distribution of Neurofilament Protein-Immunoreactive Neurons in Corticocortical Projections to Areas V1 and V2[1]

Source area	Monkeys							
	RH3	RH5	RH6	RH9	RH10	RH13	RH14	Mean
Projections to area V1								
Area MT								
Layer II–III	75.0	58.3	60.2	46.8	54.7	65.2	59.9	60.0 ± 4.1
V–VI	79.4	76.6	89.0	79.5	74.2	76.1	78.6	79.1 ± 4.2
Area V4								
Layers II–III	68.3	56.0	70.4	57.4	48.3	59.2	61.0	60.1 ± 2.8
V–VI	78.8	87.6	81.8	84.6	74.8	75.3	77.7	80.1 ± 4.4
Area V3								
Layers II–III	70.0	72.5	74.7	54.4	55.5	61.2	65.5	64.8 ± 4.0
V–VI	54.2	77.4	82.0	60.4	83.0	75.4	77.2	72.8 ± 5.2
Projections to area V2								
Area MT								
Layers II–III	53.3	77.0	59.1	59.8	53.6	66.5	63.4	61.8 ± 4.1
V–VI	79.6	78.2	75.2	81.6	86.0	77.2	78.4	79.6 ± 3.2
Area V4								
Layers II–III	60.0	62.5	63.6	71.7	60.1	64.0	65.1	63.9 ± 3.8
V–VI	79.3	79.2	74.7	86.5	78.1	85.9	75.6	79.9 ± 4.3
Area V3								
Layers II–III	71.7	80.0	79.9	55.7	51.9	63.1	68.3	67.2 ± 4.2
V–VI	78.2	77.6	80.8	74.4	69.0	83.7	72.1	76.5 ± 3.7

[1]Results represent the laminar percentages of double labeled neurons (i.e., retrogradely labeled and neurofilament protein-immunoreactive) in the projections from areas MT, V4, and V3 to the injections sites in areas V1 and V2. The mean ± S.E.M. percentages from all 7 animals is also indicated. No distinction was made between the ventral and dorsal portions of areas V4 and V3. Also there is an overall homogeneous distribution of double labeled neurons among these connections, in contrast to feedforward projections (Table 2). A few neurons projecting to both areas V2 and V1 were observed exclusively in layers V and VI of these three areas, and were consistently neurofilament protein-immunoreactive (100%). Animals are coded as in Table 1. See Results and Fig. 7 for details.

injected in areas MT and V4 resulting in less efficient retrograde labeling (Table 1). However, in view of the consistency in the percentages of double labeling patterns across animals, the possibility that differences in the proportion of neurofilament protein-containing neurons among projections may result from a lower level of retrograde transport can be ruled out.

Feedforward projections. There were large differences in percentages of double labeled projection neurons among the feedforward projections analyzed. Overall, 78.4% (2,402 out of 3,065 neurons) of the retrogradely labeled neurons projecting to area MT contained neurofilament protein immunoreactivity, whereas this value was as low as 32.1% (1,670 out of 5,209 neurons) in the projections to area V4 (Table 2; Fig. 7A). Among the projections to area MT, 100% of the retrogradely labeled cells in layer IVB and the Meynert cells in area V1 were also neurofilament protein-immunoreactive (Figs. 3A–D, 5A), whereas the projection from layer III of areas V2 and V3 contained a lower proportion of double labeled neurons compared to the projection from V1 (78 and 75%, respectively, $P < 0.001$; Table 2; Fig. 5A–C). The projection from layers V–VI of area V3 to area MT contained fewer double labeled neurons than the projection from the superficial layer (57 vs. 75%, $P < 0.005$; Table 2; Fig. 5B, C).

The projections to area V4 were characterized by a much lower content of neurofilament protein immunoreactivity than the projections to area MT ($P < 0.001$ for all of the projections analyzed, Table 2; Fig. 5C). Among the projections to area V4 the percentages of double labeled neurons was generally comparable (Table 2). The projection from layer III of area V1 to area V4, including the relatively dense population of neurons observed in the foveal representation, contained a low percentage of neurofilament protein-immunoreactive neurons (25%), while slightly higher percentages were observed in the projections from layer III of areas V2 and V3A (32 and 36%, respectively; Table 2; Fig. 5C). These trends did not reach statistical significance. It is worth noting that the neurofilament protein-immunoreactive neurons located within layers II and superficial III of area V3 were frequently retrogradely labeled following injections in area V4, indicating that this particular subpopulation of neurons, which has been used as a chemoarchitectonic landmark for occipitotemporal and inferior temporal areas (Hof and Morrison, 1995), appears to be involved in short corticocortical connections (Fig. 3I, J).

Finally, a very small population of neurons projecting to both areas V4 and MT was observed predominantly in layer III of area V3A, and an inconsistent projection to areas MT and V4 was found in some animals in layers V–VI of area V2 (not shown). The very rare neurons in area V3A that projected to both areas V4 and MT were almost all double labeled (97.1%, from a total number of 32 neurons). A low proportion of neurons in the infragranular layers of area V2 showed neurofilament protein immunoreactivity (10–20%, from a total number of 50 retrogradely labeled neurons).

Feedback projections. Interestingly, the striking differences observed in percentages of neurofilament protein-immunoreactive neurons among feedforward projections were not present in the case of feedback projections to areas V1 and V2. In all of the feedback projections analyzed, the proportion of double labeled neurons averaged 69.5% (3,712 out of 5,341 neurons) in the projections to area V1 and 71.1% (6,777 out of 9,530 neurons) in the projections to area V2 (Table 3; Fig. 7B). It should be noted, however, that all of the feedback projections, except the MT to V2 projection, differed considerably from their feedforward counterparts with respect to the presence of neurofilament protein (Fig. 7). The feedback projections from area V3 to areas V1 and V2 were significantly different in their neurofilament protein content from the V3 to V4 feedforward projection, but had similar levels of neurofilament

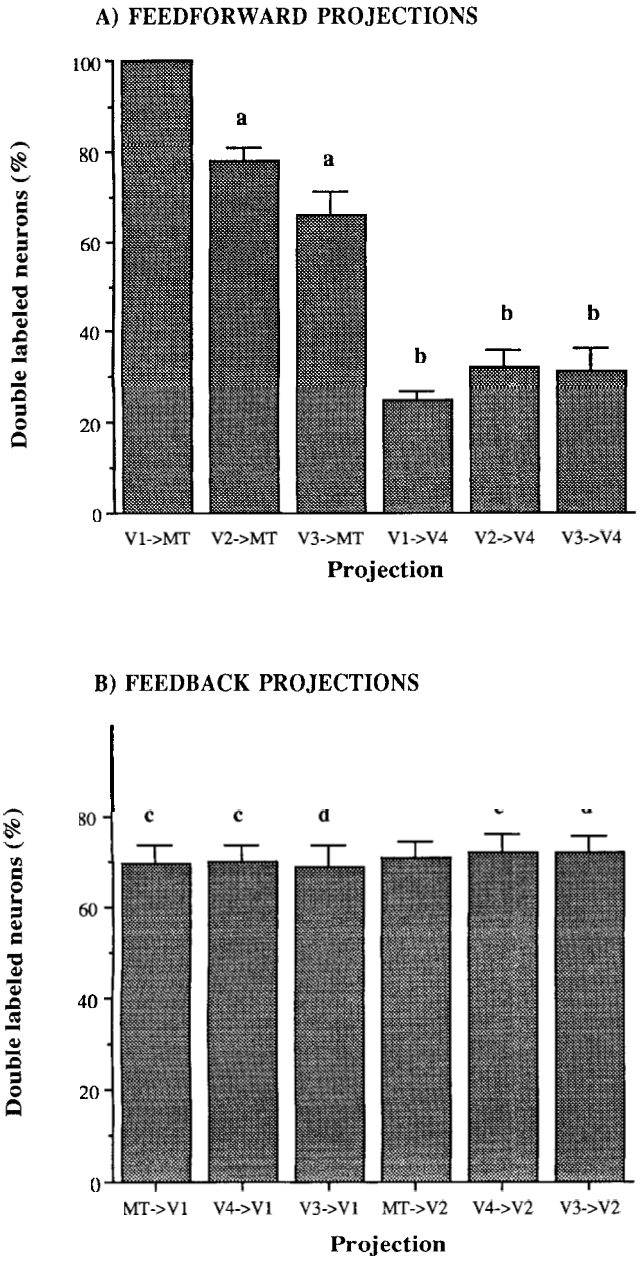

Fig. 7. Quantitative characteristics of the neurochemical phenotype of the feedforward and feedback projections analyzed in the present study. Percentages of neurofilament protein-containing neurons in feedforward projections are shown in panel **A**, and those in feedback projections in panel **B**. There are overall higher percentages in the projections to area MT than in the projections to area V4. Data from layers II–III and V–VI have been pooled in the feedforward projections from area V3 and in all feedback projections. Note the homogeneous patterns in the feedback projections. Statistically significant differences are as follows: a, $P < 0.001$ compared to the projection from area V1 to area MT; b, $P < 0.001$ compared to all of the projections to area MT; c, $P < 0.001$ compared to the corresponding feedforward projection; d, $P < 0.001$ compared to all feedforward projections to area V4. Note that feedforward and feedback connections between areas MT and V2 had comparable percentages. The projection from area V1 to area MT (100% double labeled) is significantly different from all others projections ($P < 0.001$).

protein immunoreactivity as the V3 to MT feedforward connection (Fig. 7; Tables 2, 3). Among the projections to area V1, retrogradely labeled neurofilament protein-containing neurons were more frequent in layers V–VI than in layers II–III in areas V4 and MT ($P < 0.005$; Table 3; Figs. 3K, L, 6A, B), but not in area V3 where comparable numbers of double labeled neurons were observed in supragranular and infragranular layers (Table 3; Fig. 6C). A similar observation was made for the projections to area V2 (Table 3; Fig. 6). In addition, a substantial number of neurons projecting to both areas V1 and V2 were observed in areas V3, V4, and MT (78, 123, and 145, respectively; Fig. 6). The vast majority of these neurons was located in layer VI (92%), whereas very few were found in the supragranular layers and in layer V. All of these neurons displayed neurofilament protein immunoreactivity, in a manner comparable to the feedforward neurons projecting to more than one area described above.

DISCUSSION

The present results indicate that the neurons of origin of feedforward and feedback corticocortical connections from the occipital cortex to areas MT and V4 are characterized by distinct neurochemical features. Quantitatively, the projections from areas V1, V2, and V3 to MT contain consistently higher numbers of neurofilament protein-immunoreactive neurons (78%) than the projections to area V4 (32%), whereas feedback projections from areas MT, V4, and V3 do not show such differences. Also, each projection is characterized by a specific neurofilament protein distribution profile in that all of the neurons projecting from area V1 to area MT are double labeled, whereas there is a progressive decrease in the percentages of immunoreactive neurons in the projections from areas V2 and V3. In contrast, the feedforward projections in the occipitotemporal pathway display a more homogeneous, yet lower, proportion of double labeled neurons, and the feedback projection, irrespective of their site of termination, contain homogeneously high levels of neurofilament protein (about 70%; Fig. 7). In addition, the specific regional and laminar distribution of neurofilament protein parallel these quantitative patterns.

Recent analyses of corticocortical projections have shown that overall, approximately 30% of all corticocortically projecting neurons are neurofilament protein-immunoreactive (Campbell et al., 1991; Hof et al., 1995a). Certain projections, such as those between the anterior cingulate and prefrontal cortices, are characterized by very low numbers of neurofilament protein-enriched neurons, while others, such as connections between the prefrontal and superior temporal cortices, contain as many as 90% double labeled neurons (Campbell et al., 1991; Hof et al., 1995a). The present quantitative analysis reveals that a comparable degree of variability exists in feedforward and feedback visual projections. The much higher densities of neurofilament protein-immunoreactive neurons in the projections to area MT is fairly comparable to the results obtained in a variety of long association connections linking the temporal, parietal and prefrontal cortices, whereas the percentages of double labeled neurons in the projections to area V4 are within the range of short corticocortical connections between adjacent cortical domains (Campbell et al., 1991; Hof et al., 1995a). It should be noted, however, that from the present data, the length of the cortical projection per se

does not appear to be a major determinant of the concentration of neurofilament protein. The feedforward connections to area MT and V4 and the reciprocal connections to areas V1 and V2, which have a smaller range than the long corticocortical projections described in Hof et al. (1995a), may differ in this regard from these other corticocortical pathways.

Several studies have indicated that neurofilament protein is involved in the maintenance and stabilization of the axonal cytoskeleton, and that its expression levels correlate with axonal size (Morris and Lasek, 1982; Hoffman et al., 1987; Nixon et al., 1994; Pijak et al., 1996; Xu et al., 1996). It has also been proposed that the expression and phosphorylation of the diverse neurofilament protein subunits, as well as other cytoskeletal components, during development are neuron-type specific and contribute to the formation of the adult axonal and somatodendritic cytoskeleton (Riederer et al., 1995, 1996). Similarly, the presence of high levels of nonphosphorylated neurofilament protein in the somatodendritic compartment of a relatively small number of highly specialized subsets of neocortical neurons has been proposed to be a neurochemical feature possibly related to a distinctive role of these neurons in corticocortical systems (Campbell and Morrison, 1989; De Lima et al., 1990; Campbell et al., 1991; Hof and Morrison, 1995; Hof et al., 1995a). The observed differential distribution of neurofilament protein-containing neurons in these projections may reflect differential involvement of these neurons in the detection of submodalities within a sensory map, such as color, motion, direction, and speed of movement (Hof and Morrison, 1995). Also, the presence of neurofilament protein in the perikaryon has been correlated to cell size and conduction velocity of nerve fibers (Lawson and Waddell, 1991). The high representation of neurofilament protein-immunoreactive neurons in the occipitoparietal pathway, as well as the large size of layer IVB and Meynert cells in area V1 that furnish a direct projection to area MT (Fries et al., 1985), suggest that the presence of a specialized cytoskeleton may represent an important cellular feature in neurons involved principally in the detection and analysis of motion. In this context, it is worth noting that axons of neurons projecting from area V1 to area MT are typically large (up to 3 μm in diameter), whereas axons of other visual projections are characterized by smaller diameters (0.5 to 2 μm; Rockland, 1989, 1992, 1995; Rockland and Virga, 1990; Rockland et al., 1994). Also, based on analyses of reciprocal connections between areas V1 and MT, Zeki and Shipp (1989) have proposed that Meynert neurons may be involved in the fast transfer of motion-related information to area MT which may prepare the latter area to receive a more elaborate information from layer IVB of V1 and from areas V2 or V3.

Interestingly, the largest retinal ganglion cells are enriched in neurofilament protein, as are most of the neurons in the magnocellular layers of the lateral geniculate nucleus (Straznicky et al., 1992; Vickers et al., 1995). The fact that small retinal ganglion cells, parvicellular neurons in the lateral geniculate nucleus (Vickers et al., 1995), and the cortical components of the projections to area V4 analyzed in the present study, including the connection from the foveal representation from areas V1 to V4 (Daniel and Whitteridge, 1961; Zeki, 1978; Yukie and Iwai, 1985; Nakamura et al., 1993), all display low levels of neurofilament protein immunoreactivity, demonstrates that segregation of neurochemical phenotype in the connections between occipital regions and areas MT and V4 may occurs at many levels of the visual system. It is therefore possible that projections enriched in neurofilament protein, such as the projections to area MT, perform the transfer of complex sensory information at high conduction velocities with minimal decay and high temporospatial accuracy. This is of particular interest with respect to data demonstrating that in area V1, "magnocellular" neurons are activated earlier than "parvicellular" neurons (Marrocco, 1976; Raiguel et al., 1989; Nowak et al., 1995), and that in area V2, neurons located in the cytochrome oxidase thick stripes fire about 20 ms earlier than neurons in the thin stripes (Munk et al., 1995), indicating strong differences in visual latencies among projection neurons to areas V4 and MT. These authors also reported shorter latencies in direction-selective neurons, whereas color-selective neurons show slower responses (Munk et al., 1995). It should be noted that there was no clear indication of patchiness in the distribution of neurofilament protein-containing neurons in the different cortical areas studied that may correspond to functional cortical domain. Similarly, our previous analysis of neurofilament protein immunoreactivity in the macaque monkey visual cortex did not reveal such intraregional segregation patterns (Hof and Morrison, 1995). No complete analysis of the possible correlation of neurofilament protein distribution with cytochrome oxidase domains was performed in the present analysis. However, preliminary data suggest that in area V2, neurofilament protein-containing neurons retrogradely labeled from area MT are preferentially located within the cytochrome oxidase-rich domains (Kupferschmid et al., 1992), but further analysis is needed to clarify this issue.

The present analysis involved the comparison of a limited set of visual projections and for this reason, generalization of these neurochemical data to the global set of feedforward, and feedback visual connections should be considered with caution. It is possible that the substantial differences in double labeling patterns of feedforward projections may reflect to some extent mismatches in injection sites in areas V4 and MT. This is however rather unlikely to affect significantly our results since large portion of the lateral aspect of area V4 and most of area MT were consistently injected. It also possible that our injections in area V4 included only parts of this area, since it is suspected to contain several subdivisions with different properties and connectivity (Maguire and Baizer, 1984; Steele et al., 1991). In this regard, our injections were all located within the prelunate gyrus and did not extend into prelunate sulcus, omitting the area referred to as PM by Maguire and Baizer (1984). Zeki and Shipp have also shown that there are considerable differences in the projection patterns of feedforward and feedback connections among areas V1, V2, V4, and MT (Shipp and Zeki, 1989; Zeki and Shipp, 1989a,b), with feedback patterns being generally more widespread than the origin of the corresponding feedforward projection. Additional injections in areas V1 and V2 will be necessary to characterize further the possible differences in neurochemical phenotype of neurons projecting back to the representation of the periphery of the visual field.

A wealth of studies have identified pyramidal neuron populations on the basis morphological criteria (for review see Feldman, 1984; Tömböl, 1984; DeFelipe and Fariñas, 1992). Recently, subtypes of pyramidal neurons have also

been identified in studies combining tract-tracing, intracellular filling, and immunohistochemistry or electrophysiology (Katz, 1987; Chagnac-Amitai et al., 1990; Kawaguchi, 1993; Kawaguchi and Kubota, 1996; Nimchinsky et al., 1996; Yang et al., 1996), allowing for more detailed classification criteria. In spite of some limitations, the present data indicate that significant differences exist in the neurons of origin of a variety of feedforward and feedback visual connections. Interestingly, it is has been recently shown that visual perception involves feedforward visual connections, whereas visual imagery may rely on sets of feedback projections (Ishai and Sagi, 1995; Miyashita, 1995). It is therefore possible that neurofilament protein represents a useful marker to characterize select groups of projection neurons that may have a distinctive role in visual processing. To address these issues, analyses of identified neurons, combining immunohistochemistry and electrophysiology, will be needed to clarify the function of neurofilament protein in the processing of particular submodalities of the visual stimuli. Also, cell size, axonal diameter and arborization patterns may represent important variables to characterize in greater detail the relationships between the presence of neurofilament protein and the role of these neurons in visual processing.

Finally, the high cellular specificity of neurofilament protein distribution in certain feedforward and feedback visual pathways and the preferential vulnerability of neurofilament protein-enriched neurons known to occur in neurodegenerative diseases (Hof et al., 1990b; Hof and Morrison, 1990; Vickers et al., 1992, 1994, 1995), may be related to the impairment of visuomotor function frequently observed in Alzheimer's disease (Fletcher, 1994; Mentis et al., 1996). Therefore, the selective vulnerability of the occipitoparietal visual pathway in a subgroup of Alzheimer's disease patients characterized by prominent disturbances in visuomotor tasks and posterior cortical atrophy (Hof et al., 1989, 1990a, 1993), could be related to the vulnerability of restricted subpopulations of "magnocellular" corticocortical neurons sharing this specific neurochemical phenotype.

ACKNOWLEDGMENTS

We thank W.G.M. Janssen, D.M. Blumberg, J.N. Sewell III, and R.S. Woolley for expert technical assistance, Dr. W.G. Young, H.A. Stern, S. González-Sherwin, and E.M. Gertz for software development, Dr. S.B. Kupferschmid for active participation in the early stages of the project, and Dr. E.A. Nimchinsky for critical reading of the manuscript. This work was supported in part by NIH grants AG06647 and the Human Brain Project MHDA52154 (J.H.M.), the American Health Assistance Foundation (J.H.M., P.R.H.), and CNPq (R.G.).

LITERATURE CITED

Baizer, J.S., L.G. Ungerleider, and R. Desimone (1991) Organization of visual inputs to the inferior temporal and posterior parietal cortex in macaques. J. Neurosci. *11:*168–190.

Bloom, F.E., W.G. Young, E.A. Nimchinsky, P.R. Hof, and J.H. Morrison (1996) Neuronal vulnerability and informatics in human disease. In S.H. Koslow, and M.F. Huerta (eds): Progress in Neuroinformatics, Vol. 1. Hillsdale: Lawrence Erlbaum, (in press).

Campbell, M.J., and J.H. Morrison (1989) Monoclonal antibody to neurofilament protein (SMI-32) labels a subpopulation of pyramidal neurons in the human and monkey neocortex. J. Comp. Neurol. *282:*191–205.

Campbell, M.J., P.R. Hof, and J.H. Morrison (1991) A subpopulation of primate corticocortical neurons is distinguished by somatodendritic distribution of neurofilament protein. Brain Res. *539:*133–136.

Chagnac-Amitai, Y., H.J. Luhmann, and D.A. Prince (1990) Burst generating and regular spiking layer 5 pyramidal neurons of rat neocortex have different morphological features. J. Comp. Neurol. *296:*598–613.

Daniel, P.M., and D. Whitteridge (1961) The representation of the visual field on the cerebral cortex of monkey. J. Physiol. *159:*203–221.

De Lima, A.D., T. Voigt, and J.H. Morrison (1990) Morphology of the cells within the inferior temporal gyrus that project to the prefrontal cortex in the macaque monkey. J. Comp. Neurol. *296:*159–272.

DeFelipe, J., and I. Fariñas (1992) The pyramidal neuron of the cerebral cortex: morphological and chemical characteristics of the synaptic inputs. Prog. Neurobiol. *39:*563–607.

DeYoe, E.A., and D.C. Van Essen (1988) Concurrent processing streams in monkey visual cortex. Trends Neurosci. *11:*219–226.

DeYoe, E.A., S. Hockfield, H. Garren, and D.C. Van Essen (1990) Antibody labeling of functional subdivisions in visual cortex: Cat-301 immunoreactivity in striate and extrastriate cortex of the macaque monkey. Vis. Neurosci. *5:*67–81.

DeYoe, E.A., D.J. Felleman, D.C. Van Essen, and E. McClendon (1994) Multiple processing streams in occipitotemporal visual cortex. Nature *371:*151–154.

Feldman, M.L. (1984) Morphology of neocortical pyramidal neurons. In A. Peters, and E.G. Jones (eds): Cerebral Cortex, Vol. 1, Cellular Components of the Cerebral Cortex. New York: Plenum Press, pp. 123–200.

Felleman, D.J., and D.C. Van Essen (1987) Receptive field properties of neurons in area V3 of macaque extrastriate cortex. J. Neurophysiol. *57:*889–920.

Felleman, D.J., and D.C. Van Essen (1991) Distributed hierarchical processing in the primate cerebral cortex. Cereb. Cortex *1:*1–47.

Fletcher, W.A. (1994) Ophthalmological aspects of Alzheimer's disease. Curr. Opin. Ophthalmol. *5:*38–44.

Fries, W., K. Kreizer, and H.G.J.M. Kuypers (1985) Large layer VI cells in macaque striate cortex (Meynert cells) project to both superior colliculus and prestriate visual cortex area V5. Exp. Brain Res. *58:*613–636.

Gattass, R., and C.G. Gross (1981) Visual topography of striate projection zone (MT) in posterior superior temporal sulcus of the macaque. J. Neurophysiol. *46:*621–638.

Gattass, R., A.P.B. Souza, and E. Covey (1986) Cortical visual areas of the macaque: Possible substrate for pattern recognition mechanisms. Exp. Brain Res. *11(Suppl):*1-20.

Gattass, R., A.P.B. Sousa, and C.G. Gross (1988) Visuotopic organization and extent of V3 and V4 of the macaque. J. Neurosci. *8:*1831–1845.

Gundersen, H.J.G., and E.B. Jensen (1987) The efficiency of systematic sampling in stereology and its prediction. J. Microsc. *147:*229–263.

Hendry, S.H.C., S. Hockfield, E.G. Jones, and R. McKay (1984) Monoclonal antibody that identifies subsets of neurones in the central visual system of monkey and cat. Nature *307:*267–269.

Hendry, S.H.C., E.G. Jones, S. Hockfield, and R.D.G. McKay (1988) Neuronal populations stained with the monoclonal antibody Cat-301 in the mammalian cerebral cortex and thalamus. J. Neurosci. *8:*518–542.

Hockfield, S., R.B.H. Tootell, and S. Zaremba (1990) Molecular differences among neurons reveal an organization of human visual cortex. Proc. Natl. Acad. Sci. USA *87:*3027–3031.

Hof, P.R., C. Bouras, J. Constantinidis, and J.H. Morrison (1989) Balint's syndrome in Alzheimer's disease: Specific disruption of the occipitoparietal visual pathway. Brain Res. *493:*368–375.

Hof, P.R., C. Bouras, J. Constantinidis, and J.H. Morrison (1990a) Selective disconnection of specific visual association pathways in cases of Alzheimer's disease presenting with Balint's syndrome. J. Neuropathol. Exp. Neurol. *49:*168–184.

Hof, P.R., K. Cox, and J.H. Morrison (1990b) Quantitative analysis of a vulnerable subset of pyramidal neurons in Alzheimer's disease: I. Superior and inferior temporal cortex. J. Comp. Neurol. *301:*44–54.

Hof, P.R., and J.H. Morrison (1990) Quantitative analysis of a vulnerable subset of pyramidal neurons in Alzheimer's disease: II. Primary and secondary visual cortex. J. Comp. Neurol. *301:*55–64.

Hof, P.R., and E.A. Nimchinsky (1992) Regional distribution of neurofilament and calcium-binding proteins in the cingulate cortex of the macaque monkey. Cereb. Cortex *2:*456–467.

Hof, P.R., N. Archin, A.P. Osmand, J.H. Dougherty, C. Wells, C. Bouras, and J.H. Morrison (1993) Posterior cortical atrophy in Alzheimer's disease:

Analysis of a new case and re-evaluation of an historical report. Acta Neuropathol. *86:*115–223.

Hof, P.R., L.G. Ungerleider, M.J. Webster, M. Adams, and J.H. Morrison (1994) Neurofilament protein and glutamate receptor subunit proteins define subsets of corticocortical projections in the monkey visual cortex. Invest. Ophthalmol. Vis. Sci. *35:*1971.

Hof, P.R., and J.H. Morrison (1995) Neurofilament protein defines regional patterns of cortical organization in the macaque monkey visual system: A quantitative immunohistochemical analysis. J. Comp. Neurol. *352:*161–186.

Hof, P.R., E.A. Nimchinsky, and J.H. Morrison (1995a) Neurochemical phenotype of corticocortical connections in the macaque monkey: Quantitative analysis of a subset of neurofilament protein-immunoreactive projection neurons in frontal, parietal, temporal, and cingulate cortices. J. Comp. Neurol. *362:*109–133.

Hof, P.R., L.G. Ungerleider, M.J. Webster, R. Gattass, M.M. Adams, C.A. Sailstad, W.G.M. Janssen, and J.H. Morrison (1995b) Feedforward and feedback corticocortical projections in the monkey visual system display differential neurochemical phenotype. Soc. Neurosci. Abstr. *21:*904.

Hoffman, P.N., D.W. Cleveland, J.W. Griffin, P.W. Landes, N.J. Cowan, and D.L. Price (1987) Neurofilament gene expression: A major determinant of axonal caliber. Proc. Natl. Acad. Sci. USA *84:*3472–3476.

Ishai, A., and D. Sagi (1995) Common mechanisms of visual imagery and perception. Science *268:*1772–1774.

Katz, L.C. (1987) Local circuitry of identified projection neurons in cat visual cortex brain slices. J. Neurosci. *7:*1123–1149.

Kawaguchi, Y. (1993) Grouping of nonpyramidal and pyramidal cells with specific physiological and morphological characteristics in rat frontal cortex. J. Neurophysiol. *69:*416–431.

Kawaguchi, Y., and Y. Kubota (1996) Physiological and morphological identification of somatostatin- or vasoactive intestinal polypeptide-containing cells among GABAergic cell subtypes in rat frontal cortex. J. Neurosci. *16:*2701–2715.

Kupferschmid, S.B., P.R. Hof, and J.H. Morrison (1991) Corticocortical connections in macaque visual cortex exhibit differential patterns of neurofilament protein distribution. Soc. Neurosci. Abstr. *17:*845.

Kupferschmid, S.B., R. Gattass, L.G. Ungerleider, and J.H. Morrison (1992) Cytoskeletal profile of neurons involved in the M and P pathways of the macaque visual cortex. Soc. Neurosci. Abstr. *18:*389.

Kuypers, H.G.J.M., and A.M. Huisman (1984) Fluorescent tracers. In S. Fedoroff (ed): Advances in Cellular Neurobiology, Vol. 5. Orlando, FL: Academic Press, pp. 307–340.

Lawson, S.N., and J.P. Waddell (1991) Soma neurofilament immunoreactivity is related to cell size and fibre conduction velocity in rat primary sensory neurons. J. Physiol. *435:*41–63.

Lee, V.M.Y., L. Otvos Jr, M.J. Carden, M. Hollosi, B. Dietzschold, and R.A. Lazzarini (1988) Identification of the major multiphosphorylation site in mammalian neurofilaments. Proc. Natl. Acad. Sci. USA *85:*1998–2002.

Livingstone, M., and D. Hubel (1988) Segregation of form, color, movement, and depth: Anatomy, physiology, and perception. Science *240:*740–749.

Maguire, W.M., and J.S. Baizer (1984) Visuotopic organization of the prelunate gyrus in rhesus monkey. J. Neurosci. *4:*1690–1704.

Marrocco, R.T. (1976) Sustained and transient cells in monkey lateral geniculate nucleus: Conduction velocities and response properties. J. Neurophysiol. *39:*340–353.

Maunsell, J.H.R., and W.T. Newsome (1987) Visual processing in monkey extrastriate cortex. Annu. Rev. Neurosci. *10:*363–401.

Mentis, M.J., B. Horwitz, C.L. Grady, G.E. Alexander, J.W. VanMeter, J.M. Maisog, P. Pietrini, M.B. Schapiro, and S.I. Rapoport (1996) Visual cortical dysfunction in Alzheimer's disease evaluated with a temporaly graded "stress test" during PET. Am. J. Psychiatry *153:*32–40.

Mishkin, M., L.G. Ungerleider, and K.A. Macko (1983) Object vision and spatial vision: Two cortical pathways. Trends Neurosci. *6:*414–417.

Miyashita, Y. (1995) How the brain creates imagery: Projection to primary visual cortex. Science *268:*1719–1720.

Morel, A., and J. Bullier (1990) Anatomical segregation of two cortical visual pathways in the macaque monkey. Vis. Neurosci. *4:*555–578.

Morris, J.R., and R.J. Lasek (1982) Stable polymers of the axonal cytoskeleton: The axoplasmic ghost. J. Cell Biol. *92:*192–198.

Munk, M.H.J., L.G. Nowak, N. Chounlamountri, and J. Bullier (1995) Visual latencies in cytochrome oxidase bands of macaque area V2. Proc. Natl. Acad. Sci. USA *92:*988–992.

Nakamura, H., R. Gattass, R. Desimone, and L.G. Ungerleider (1993) The modular organization of projections from areas V1 and V2 to areas V4 and TEO in macaques. J. Neurosci. *13:*3681–3691.

Nimchinsky, E.A., P.R. Hof, W.G. Young, J.H. Morrison (1996) Neurochemical, morphologic and laminar characterization of cortical projection neurons in the cingulate motor areas of the macaque monkey. J. Comp. Neurol. *374:*136-160.

Nixon, R.A., P.A. Paskevich, R.K. Sihag, and C.Y. Thayer (1994) Phosphorylation on carboxyl terminus domains of neurofilament proteins in retinal ganglion cell neurons in vivo: Influences on regional neurofilament accumulation, interneuronal spacing, and axonal caliber. J. Cell Biol. *126:*1031–1046.

Nowak, L.G., M.H.J. Munk, P. Girard, and J. Bullier (1995) Visual latencies in areas V1 and V2 of the macaque monkey. Vis. Neurosci. *12:*371–384.

Peters, A. (1994) The organization of the primary visual cortex in the macaque. In A. Peters, K.S. Rockland (eds): Cerebral Cortex, Vol. 10, Primary Visual Cortex in Primates. New York: Plenum Press, pp. 1–35.

Peters, A., and C. Sethares (1991) Organization of pyramidal neurons in area 17 of monkey visual cortex. J. Comp. Neurol. *306:*1–23.

Peters, A., and E. Yilmaz (1993) Neuronal organization in area 17 of cat visual cortex. Cereb. Cortex *3:*49–68.

Pijak, D.S., G.F. Hall, P.J. Tenicki, A.S. Boulos, D.I. Lurie, and M.S. Selzer (1996) Neurofilament spacing, phosphorylation, and axon diameter in regenerating and uninjured lamprey axons. J. Comp. Neurol. *368:*569–581.

Raiguel, S.E., L. Lagae, B. Gulyas, and G. Orban (1989) Response latencies of visual cells in macaque areas V1, V2, and V5. Brain Res. *493:*155–159.

Riederer, B.M., E. Draberova, V. Viklicky, and P. Draber (1995) Changes of MAP2 phosphorylation during brain development. J. Histochem. Cytochem. *43:*1269–1284.

Riederer, B.M., R. Porchet, and R.A. Marugg (1996) Differential expression and modification of neurofilament triplet proteins during cat cerebellar development. J. Comp. Neurol. *364:*704–717.

Rockland, K.S. (1989) Bistratified distribution of terminal arbors of individual axons projecting from area V1 to middle temporal area (MT) in the macaque monkey. Vis. Neurosci. *3:*155–170.

Rockland, K.S. (1992) Configuration, in serial reconstruction, of individual axons projecting from area V2 to V4 in the macaque monkey. Cereb. Cortex *2:*353–374.

Rockland, K.S. (1995) Morphology of individual axons projecting from area V2 to MT in the macaque. J. Comp. Neurol. *355:*15–26.

Rockland, K.S., and D.N. Pandya (1979) Laminar origins and terminations of cortical connections of the occipital lobe in the rhesus monkey. Brain Res. *179:*3–20.

Rockland, K.S., and A. Virga (1990) Organization of individual cortical axons projecting from area V1 (area 17) to V2 (area 18) in the macaque monkey. Vis. Neurosci. *4:*11–28.

Rockland, K.S., K.S. Saleem, and K. Tanaka (1994) Divergent feedback connections from areas V4 and TEO in the macaque. Vis. Neurosci. *11:*579–600.

Sachs, L. (1984) Applied Statistics — A Handbook of Techniques, second edition. New York: Springer.

Shipp, S., and S. Zeki (1989a) The organization of connections between areas V5 and V1 in macaque monkey visual cortex. Eur. J. Neurosci. *1:*309–332.

Shipp, S., and S. Zeki (1989b) The organization of connections between areas V5 and V2 in macaque monkey visual cortex. Eur. J. Neurosci. *1:*333–354.

Steele, G.E., R.E. Weller, and C.G. Cusick (1991) Cortical connections of the caudal subdivisions of the dorsolateral area (V4) in monkeys. J. Comp. Neurol. *306:*495–520.

Sterio, D.C. (1984) The unbiased estimation of number and sizes of arbitrary particles using the disector. J. Microsc. *134:*127–136.

Sternberger, L.A., and N. Sternberger (1983) Monoclonal antibodies distinguish phosphorylated and nonphosphorylated forms of neurofilaments in situ. Proc. Natl. Acad. Sci. USA *80:*6126–6130.

Straznicky, C., J.C. Vickers, R. Gábriel, and M. Costa (1992) A neurofilament protein antibody selectively labels a large ganglion cell type in the human retina. Brain Res. *582:*123–128.

Tömböl, T. (1984) Layer VI cells. In A. Peters, and E.G. Jones (eds): Cerebral Cortex, Vol. 1, Cellular Components of the Cerebral Cortex. New York: Plenum, pp. 479–519.

Ungerleider, L.G., and M. Mishkin (1979) The striate projection zone in the superior temporal sulcus of *Macaca mulatta:* Location and topographic organization. J. Comp. Neurol. *188:*347–366.

Ungerleider, L.G., and R. Desimone (1986) Cortical connections of the visual area MT in the macaque. J. Comp. Neurol. *248:*190–222.

Van Essen, D.C., J.H.R. Maunsell, and J.L. Bixby (1981) The middle temporal visual area in the macaque: Myeloarchitecture, connections, functional properties and topographic connections. J. Comp. Neurol. *199:*293–326.

Van Essen, D.C., and J.L. Gallant (1994) Neural mechanisms of form and motion processing in the primate visual system. Neuron *13:*1–10.

Vickers, J.C., A. Delacourte, and J.H. Morrison (1992) Progressive transformation of the cytoskeleton associated with normal aging and Alzheimer's disease. Brain Res. *594:*273–278.

Vickers, J.C., J.H. Morrison, V.L. Friedrich Jr, G.A. Elder, D.P. Perl, R.N. Katz, and R.A. Lazzarini (1994) Age-associated and cell-type-specific neurofibrillary pathology in transgenic mice expressing the human midsized neurofilament subunit. J. Neurosci. *14:*5603–5612.

Vickers, J.C., R.A. Schumer, S.M. Podos, R.F. Wang, B.M. Riederer, and J.H. Morrison (1995) Differential vulnerability of neurochemically identified subpopulations of retinal neurons in a monkey model of glaucoma. Brain Res. *680:*23–35.

West, M.J., L. Slomianka, and H.J.G. Gundersen (1991) Unbiased stereological estimation of the total number of neurons in the subdivisions of the rat hippocampus using the optical fractionator. Anat. Rec. *231:*482–497.

Xu, Z., J.R. Marszalek, M.K. Lee, P.C. Wong, J. Folmer, T.O. Crawford, S.T. Hsieh, J.W. Griffin, and D.W. Cleveland (1996) Subunit composition of neurofilaments specifies axonal diameter. J. Cell Biol. *133:*1061–1069.

Yang, C.R., J.K. Seameans, and N. Gorelova (1996) Electrophysiological and morphological properties of layers V-VI principal pyramidal cells in rat prefrontal cortex in vitro. J. Neurosci. *16:*1904–1921.

Young, W.G., E.A. Nimchinsky, P.R. Hof, F.E. Bloom, and J.H. Morrison (1995) NeuroZoom: Computer software for quantitative neuroanatomic mapping and stereology. Soc. Neurosci. Abstr. *21:*1078.

Yukie, M., and E. Iwai (1985) Laminar origin of direct projection from cortex area V1 to V4 in the rhesus monkey. Brain Res. *346:*383–386.

Zeki, S.M. (1974) Functional organization of a visual area in the posterior bank of the superior temporal sulcus of the rhesus monkey. J. Physiol. *236:*549–573.

Zeki, S.M. (1978) The cortical projections of foveal striate cortex in the rhesus monkey. J. Physiol. *277:*227–244.

Zeki, S., and S. Shipp (1988) The functional logic of cortical connections. Nature *335:*311–317.

Zeki, S., and S. Shipp (1989) Modular connections between areas V2 and V4 of macaque monkey visual cortex. Eur. J. Neurosci. *1:*494–506.